P. Pagano[1], D. Mackay[1], A. Yeates[2]

1 University of St Andrews
2 Durham Univesity
pp25@st-andrews.ac.uk

Technique for observation derived boundary conditions for Space Weather

Abstract

We propose a new efficient and accurate modelling technique suitable for the next generation of Space Weather predictive tools. Specifically, we put forward an approach that can provide interplanetary Space Weather forecasting models with an accurate time dependent boundary condition of erupting flux ropes in the upper Solar Corona. The unique strength of this technique is that it follows the time evolution of coronal magnetic fields directly driven from observations and captures the full life span of magnetic flux ropes from formation to ejection. To produce accurate and effective boundary conditions we couple two different modelling techniques, MHD simulations with quasi-static non-potential modelling. Our modelling approach uses a time series of observed synoptic magnetograms to drive the non potential evolution model of the coronal magnetic field to follow the formation and loss of equilibrium of magnetic flux ropes. Following this a MHD simulation captures the dynamic evolution of the ejection phase of the flux rope into interplanetary space. We focus here on the MHD simulation that describe the ejection of two magnetic flux ropes through the solar corona to the outer boundary. At this boundary we then produce time dependent boundary conditions for the magnetic field and plasma that in the future may be applied to interplanetary space weather prediction models. We illustrate that the coupling of observationally derived quasi-static non-potential magnetic field modelling and MHD simulations can significantly reduce the computational time for producing realistic observationally derived boundary conditions at the boundary between the corona and interplanetary space.

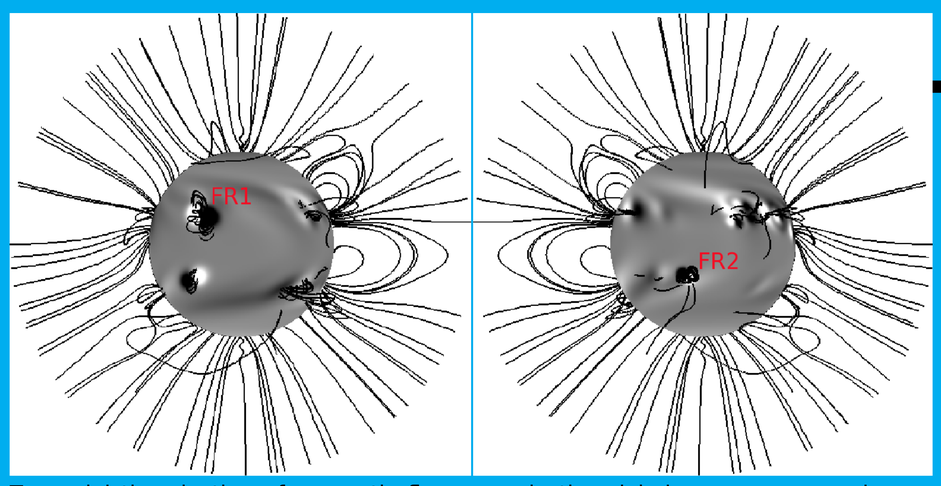

To model the ejection of magnetic flux ropes in the global corona, we employ a dual modelling technique of MHD simulations coupled with a quasi static non-potential global model (Yeates et al., 2010). This approach is an extension of Pagano et al. 2013. In this way we follow the slow build-up of stress in the magnetic field under observed solar timescales (days -months) along with the dynamic eruption timescale (min-hours). We use the magnetic configuration obtained from a simulation of the Cycle 23 (Yeates and Mackay, 2012), where the structure of the corona was produced by the effects of differential rotation, meridional flow, surface magnetic diffusion and magnetic flux emergence. We select a snapshot of the global non-potential model where two isolated flux ropes have formed (FR1 and FR2) with enough stress accumulated and likely to erupt.

MHD simulation

$$\frac{\partial \rho}{\partial t} + \boldsymbol{\nabla} \cdot (\rho \boldsymbol{v}) = 0,$$

$$\frac{\partial \rho \boldsymbol{v}}{\partial t} + \boldsymbol{\nabla} \cdot (\rho \boldsymbol{v}\boldsymbol{v}) + \nabla p - \frac{(\boldsymbol{\nabla} \times \boldsymbol{B}) \times \boldsymbol{B})}{4\pi} = \rho \boldsymbol{g},$$

$$\frac{\partial \boldsymbol{B}}{\partial t} - \boldsymbol{\nabla} \times (\boldsymbol{v} \times \boldsymbol{B}) = 0,$$

$$\frac{\partial e}{\partial t} + \boldsymbol{\nabla} \cdot [(e + p)\boldsymbol{v}] = \rho \boldsymbol{g} \cdot \boldsymbol{v},$$

MPI-AMRVAC software (Porth et al. 2014) to solve MHD with gravity as source term.
Domain with 256x256x512 cells uniformly spaced and it extends over 3 solar radii in the radial direction, from θ=0.75° to θ=179.25° in co-latitude, and 360° in longitude ϕ.
The boundary conditions are treated with ghost cells: open boundary conditions at the outer boundary, fixed at the lower boundary, reflective boundary at the θ boundaries and periodic at the ϕ boundaries.

Strategy and initial conditions

$$\omega = \sqrt{\omega_r^2 + \omega_\theta^2 + \omega_\phi^2}$$

$$\omega_r = \frac{|B \times \nabla B_r|^2}{|\nabla B_r|^2} \qquad \omega_\theta = \frac{|B \times \nabla B_\theta|^2}{|\nabla B_\theta|^2} \qquad \omega_\phi = \frac{|B \times \nabla B_\phi|^2}{|\nabla B_\phi|^2}$$

To produce a complete set of MHD variables we need plasma density, velocity and temperature. We aim to take into account the heterogeneity of the solar corona (i.e. dense active regions and less dense quiet Sun regions) and horizontal magnetic field structures (such as prominences or filaments), generally two orders of magnitude cooler and denser than the ambient corona. Thus, we use ω, that is positive definite and peaks where the magnetic field exhibits a complex twisted field, e.g. near the axis of a magnetic flux rope, and that is proportional to the magnetic field intensity, thus higher near the solar surface (where the magnetic field is more intense).

$$T = \Omega(T_{fluxrope} - T_{corona}) + T_{corona}$$

$$p = \frac{\rho_{LB}}{\mu m_p} k_B 2 T_{corona} \exp\left(-\frac{M_\odot G \mu m_p}{2 T_{corona} k_B R_\odot}\right) \exp\left(\frac{M_\odot G \mu m_p}{2 T_{corona} k_B r}\right)$$

The temperature is bound between T_{corona} and $T_{fluxrope}$ by Ω, which is a function of ω. The thermal pressure is specified by the solution for hydro-static equilibrium with a uniform temperature set equal to T_{corona}. The density is derived by T and p with the equation of state.

The maps of density and temperature show that regions with a more complex magnetic configuration are denser and cooler. The magnetic flux ropes appear as regions with density and temperature one or two orders of magnitude denser and colder than the surrounding ambient values and the initial conditions produce an inhomogeneous corona.

The initial plasma β in the simulation ranges between $\beta=10^{-3}$ at the flux ropes to β=1 in confined regions where the magnetic field is weak. Due to the low β values at the flux ropes, the strongest unbalanced force in the initial condition is the radially directly Lorentz force at these locations.
In addition to the unbalanced Lorentz force the radial profile of density and pressure also does not prescribe a balance between the thermal pressure gradient and gravity.

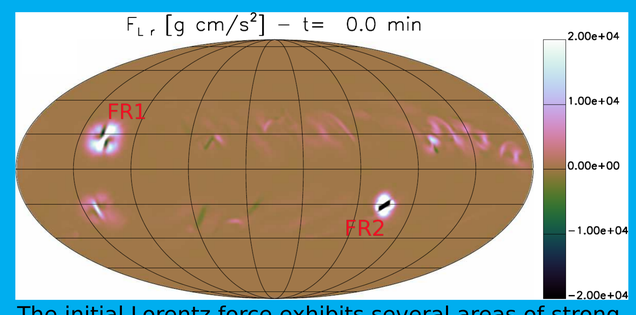

The initial Lorentz force exhibits several areas of strong outward radial force. Two show a significantly larger positive Lorentz force. One in the Northern Hemisphere and one in the Southern Hemisphere. These occur where large flux ropes have formed and can no longer be fully contained by the overlying fields. Outside of flux ropes lie regions of positive or negative radial component of Lorentz force can be seen.

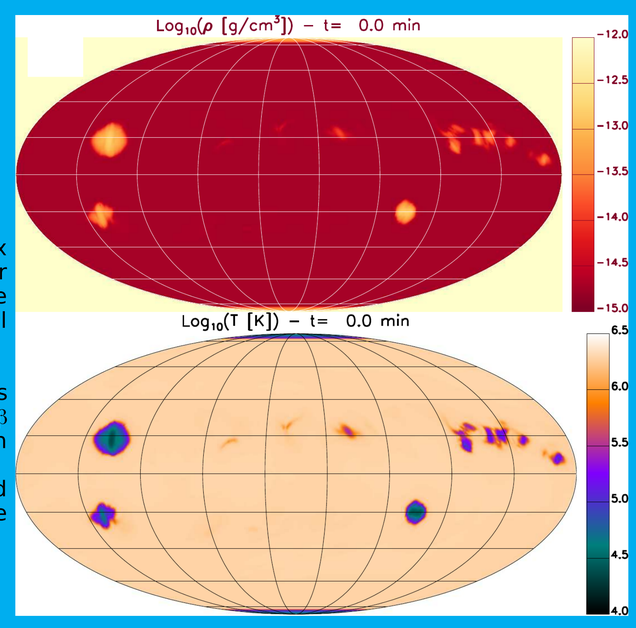

Flux rope ejections

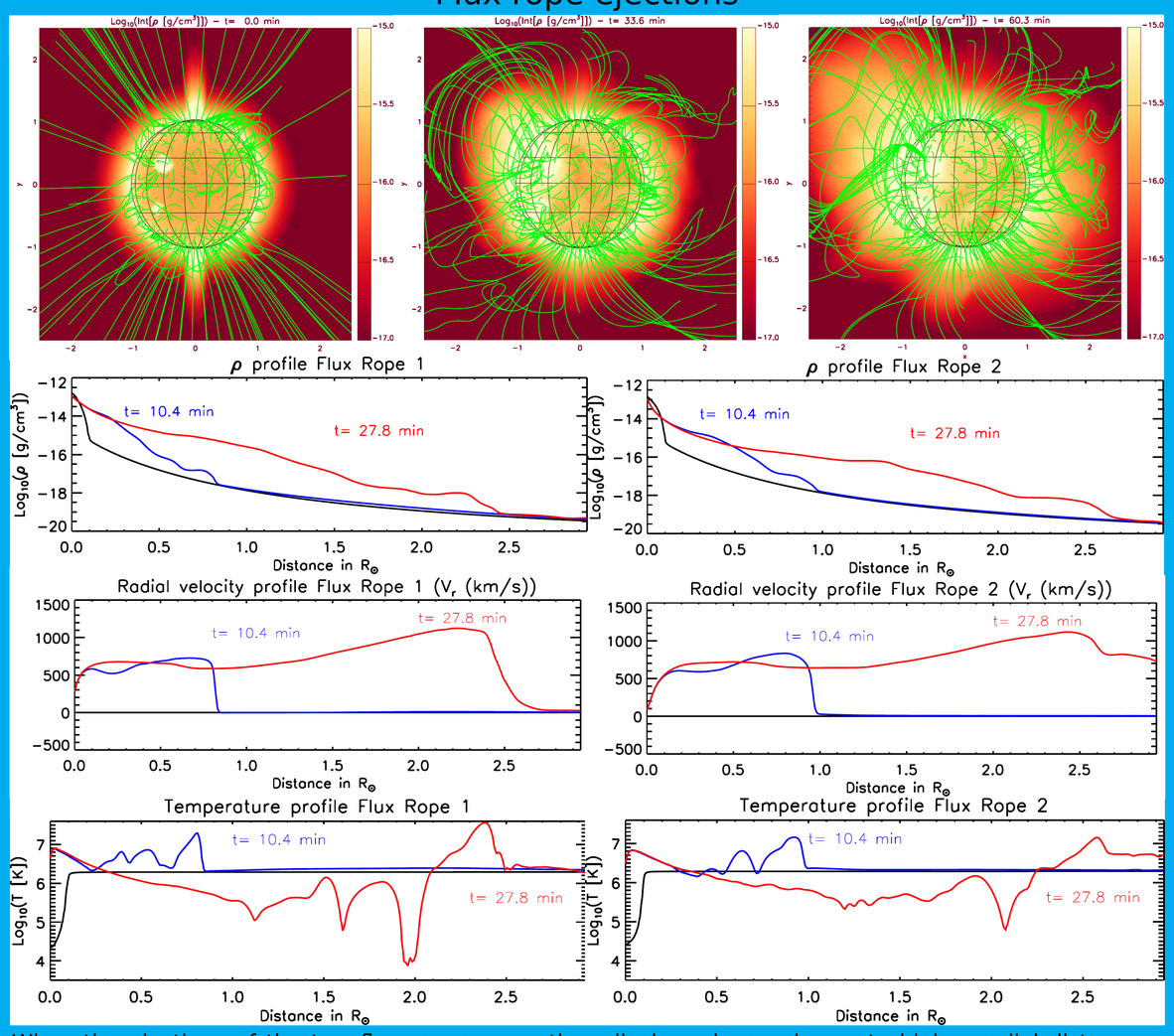

When the ejections of the two flux ropes occur they displace dense plasma to higher radial distances, which results in an increased column density around the locations of each flux rope: two circular structures expanding at either limbs, one towards North and the other towards South. During the ejections the global magnetic field undergoes a rapid evolution. After t=60.3 min two circular expanding structures of density have expanded sufficiently that they cross the outer boundary of the domain.

Radial cuts of density, temperature and radial velocity from the photospheric boundary to the outer boundary (black lines show initial profiles) show the dense flux rope travelling from low heights along with the stratified atmosphere. At later times the presence of the ejection is identified by an excess in density compared to that of the background stratified atmosphere. At t=10.4 min the density excess of the ejected plasma has reached 0.8 RSUN for FR1 and 1 RSUN for FR2 showing that they are traveling at different speeds. Structures of FR2 travel about 20% faster than the same structures of FR1.
At the lead front of the density excess there is a very sharp temperature increase to 107 K and behind the front the temperature profile also shows significant structure, where at t=10.4 min the temperature profile in the atmosphere exhibits a dip at the location of the axis of both FR1 (0.2 RSUN) and FR2 (0.4 RSUN). At t=10.4 min the radial velocity profiles for both FR1 and FR2 exhibit a very similar behaviour, where there is an initial sharp rise at the photosphere, followed by a slight dip before becoming roughly level. The ejection of both flux ropes can be characterized by a front (density excess, sharp increase in temperature and radial velocity) and a core (density excess, temperature dip, slower than the front). Overall, the two ejections show similar structures, but different properties that lead to increasingly different ejections.

Space Weather

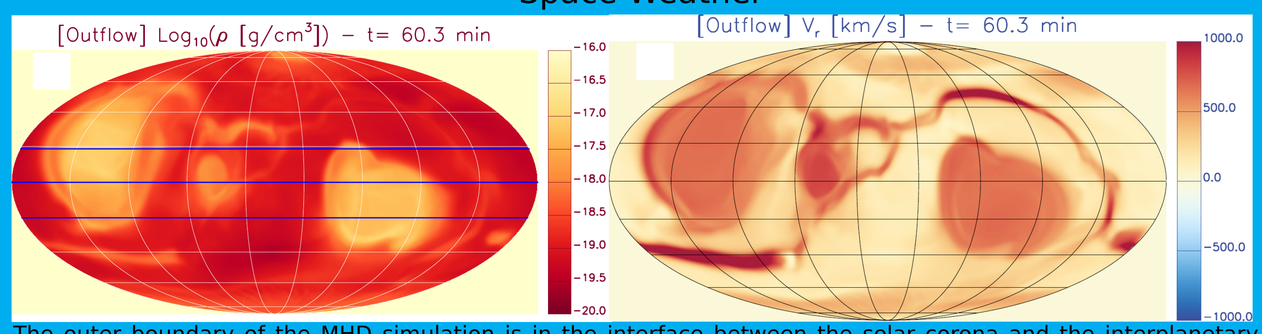

The outer boundary of the MHD simulation is in the interface between the solar corona and the interplanetary space and the plasma and and magnetic field crossing it are injected in the Space Weather.
The two flux rope ejections appear as density excesses covering an area of some tens of squared degrees where FR1 involves a wider area than FR2. They predominately lie in one hemisphere but both straddle the equator and show internal variations in the density which are specific for each flux rope. The same regions exhibit an outward velocity in the order of hundreds of km/s. Outside the region corresponding to the erupting flux ropes the corona has a significantly smaller outward velocity and the fastest speeds are found along the polar inversion line (1000 km/s). The internal structure of the radial velocity patterns differs as well.

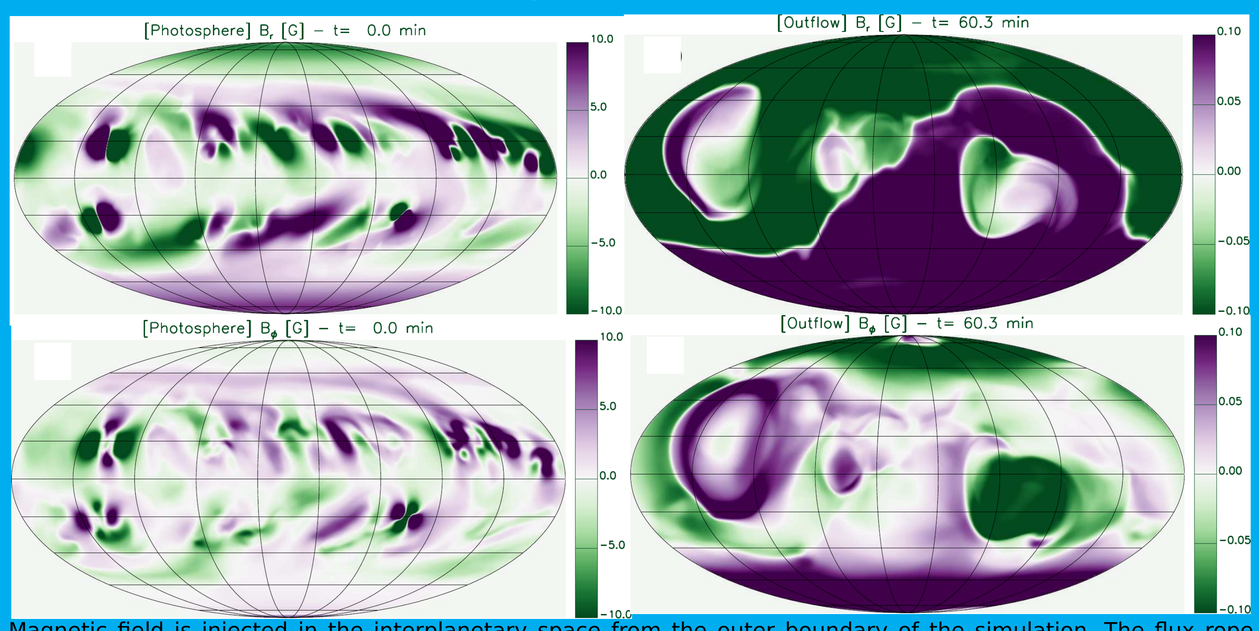

Magnetic field is injected in the interplanetary space from the outer boundary of the simulation. The flux rope magnetic field significantly perturbs this boundary. The radial component of the magnetic field exhibits a distribution where two regions with opposite polarity are separated by a PIL. Both erupting flux ropes carry a negative θ component (not shown). In Bφ, two visible regions are present: around FR1 a distinct ring structure of positive Bφ and at FR2 there is a uniform negative Bφ. There is no evident correlation between the magnetic field at the lower boundary when the ejections start and at the outer boundary, e.g. i) from the many visible features only two reach the outer boundary, ii) the flux rope PILs at the outer boundary are different in shape and size even if originating from similar flux ropes, iii) both show a negative Bθ region at the outer boundary with different Bφ structures, showing different rotations. Thus within the present simulation due to the low coronal properties of the field and the regions in which the flux ropes form we find significant differences in the field distribution at the outer boundary. If the low coronal field is not accurately modelled than such variation in ICM's will not be taken into account.

References:
Pagano, P., Mackay, D. H., & Poedts, S. 2013, A&A, 560, A38
Porth, O., Xia, C., Hendrix, T., Moschou, S. P., & Keppens, R. 2014, ApJS, 214, 4
Yeates, A. R. & Mackay, D. H. 2012, ApJ, 753, L34
Yeates, A. R., Attrill, G. D. R., Nandy, D., et al. 2010a, ApJ, 709, 1238